Temperature Sensing with Passive Ceramic RFID Tag

Dmitry Dobrykh
School of Electrical Engineering
Tel Aviv University
Tel-Aviv, Israel
Israel dmitryd@mail.tau.ac.il

Alyona Maksimenko
School of Physics and Engineering,
ITMO University
Saint Petersburg, Russia
alyona.maksimenko@metalab.ifmo.ru

Ildar Yusupov
School of Physics and Engineering,
ITMO University
Saint Petersburg, Russia
ildar.yusupov@metalab.ifmo.ru

Mikhail Udrov
School of Physics and Engineering,
ITMO University
Saint Petersburg, Russia
mikhail.udrov@metalab.ifmo.ru

***Abstract*— Radio frequency identification is a wireless technology that allows contactless readout of data from a passive device through time-modulated backscattering. High epsilon ceramic resonators, capable of shrinking interaction volumes by orders of magnitude, open new possibilities for developing long-range compact tags. Here we demonstrate that this technology also allows for accurate tracking after environmental temperature changes without an additional sensing circuit. Several material platforms, demonstrating significant permittivity temperature dependence, were explored and demonstrated less than a 1°C sensitivity. Specifically, the passive tag, based on $BaTiO_3$ with ε=500 and interrogated from a 4-meter distance, was demonstrated. Equipping high-index ceramic RFID tags with additional capabilities apart from their long reading ranges further promotes this technology in application to the Internet of Small Things, where small low-cost low-resource entities are foreseen to perform multiple functions.**

Keywords — RFID, dielectric resonators, sensors

I. INTRODUCTION

The technology of radio-frequency identification (RFID) is now ubiquitous and extensively employed technology across various applied fields such as retail, healthcare, logistics, and many others [1]. While various RFID setups are in use, the UHF (ultra-high frequency) configuration provides an optimal balance between cost and operational efficiency. Tags in this configuration consist of an antenna and a built-in chip that extracts power from the rectified energy of incoming high-frequency signals [2]. The data readout process begins when a reader device queries the tag, prompting it to return a time-modulated signal. This type of communication channel allows to capture of the tag's unique identification number and, with more advanced architectures, to retrieve additional information, e.g., real-time sensing data.

The idea of the Internet of Things (IoT) in the context of Industry 4.0 is driving the development of wireless technologies, which should be high-performance yet cost-effective [3], [4]. RFID is recognized as one of the key technologies for this purpose. RFID sensors have been proven to be effective in monitoring various parameters such as temperature [5], humidity [6], pressure [7], pest presence [8], and others. Most RFID sensors come with an external or chip-integrated sensor that is specifically designed to track a particular parameter and may require a battery. In some alternative realizations, additional expensive equipment is necessary.

The objective of this work is to introduce a high-permittivity dielectric tag that can detect temperature changes without the need for additional sensing microchips. The long-range passive ceramic RFID tag performs sensing by relying on a strong temperature-dependent response of the ceramic resonator and the multi-channel property of the RFID communication protocol. The ceramic resonator supports a high-quality factor magnetic dipole mode, which occupies a single among 50 available communication channels within the designated RFID bandwidth. For instance, in the United States, the UHF RFID band operates at 902-928 MHz, with 50 channels of 500 KHz each [2]. Frequency hopping between channels allows for anti-collision protocols that enable the simultaneous interrogation of multiple tags and prevent adjacent readers from interfering with each other. By monitoring the readout channel, which follows the resonant frequency of the tag, the temperature change is measured without any additional equipment. This concept is illustrated in Fig. 1.

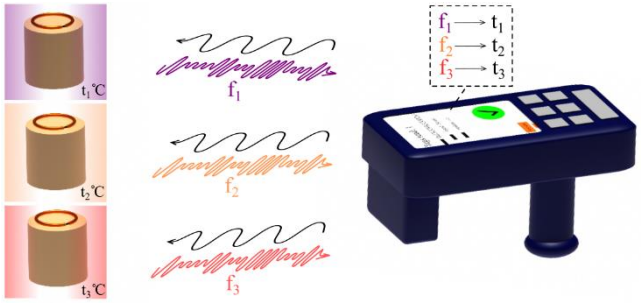

Fig. 1. Temperature sensing principle of passive ceramic RFID tag. The change in the temperature is imprinted on the communication channel within the RFID bandwidth. Apart from the tag's ID, the reader also records the communication channel number, thus allowing for retrieval of the temperature information

The key component of the tag's architecture is a ceramic resonator with high dielectric permittivity. The cylindrical resonator supports localized fundamental magnetic dipole

The fabrication of ceramic resonators and numerical simulations of this work were supported by the Russian Science Foundation (Project 23-19-00511). There is no joint funding between the teams for the project, which started at 2021.

mode TE01. To enable the RFID tag's operation, the chip was soldered into the gap of a metal ring. This ring was positioned above the ceramic cylinder. The inductive coupling between the resonator and the ring facilitated the activation and readout of the tag. In more detail, the geometry and operational principle of ceramic RFID tags developed by our team have been reported in [9]–[12].

II. Numerical Model

The proposed tag geometry is presented in Fig. 2*a*, and the parameters of the ceramic tag are listed in Table I.

TABLE I. Parameters of the Ceramic Tag

Radius of the resonator, R	7.3 mm
Height of the resonator, h	11 mm
Dielectric permittivity of the resonator, ε_r	506
Loss tangent $tan\delta$	0.0004
Split ring radius, R_{ring}	3 mm

This configuration allows operation within the 865-868 MHz range, corresponding to the European EPCGEN2 UHF RFID frequency standard. The numerical analysis was performed using CST Studio Suite. A metal ring, characterized by an impedance of $Z = 14.1 - j147.8$, initiates excitation of the resonator's magnetic dipole mode. This impedance aligns with the that of the Monza R6 chip as specified in the datasheet. Impedance matching is accomplished purely through adjustments to the ring's geometry and its inductive interaction, without requiring any additional components.

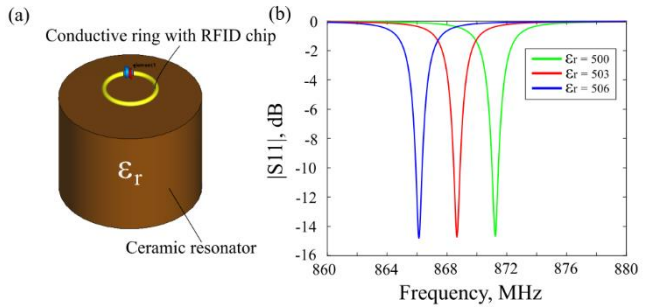

Fig. 2. (a) Layout of the ceramic RFID tag. (b) Numerical $|S_{11}|$ spectra of the ceramic tag for several resonator permittivity values

The results of the numerical |S11| spectra calculations for the optimized geometry at three varying dielectric permittivity levels are illustrated in Fig. 2*b*. The results indicate that a small change in the permittivity (less than 1 %) can result in a significant shift in resonance. This makes it possible to create a temperature sensor tag that is highly sensitive.

III. Temperature Measurements with Ceramic Resonators

Experimental measurements were carried out to determine the effectiveness of ceramic tags under different temperatures. We produced a set of cylindrical dielectric resonators with permittivities of 80, 100, 270, and 500. We selected the geometric parameters of each resonator so that the TE01 mode would fall within the UHF RFID communication range. A Rohde & Schwarz ZVB20 vector network analyzer with a small loop antenna connected to one of the analyzer's ports was used to measure the resonant frequency of the TE01 mode of dielectric resonator (Figure 3a). Inset in Figure 3a shows the images of the resonators that were fabricated. The measurements were performed across a temperature range of 40 to 90°C. To heat the resonators, we used a plate and an industrial fan, while temperature control was performed using a thermocouple.

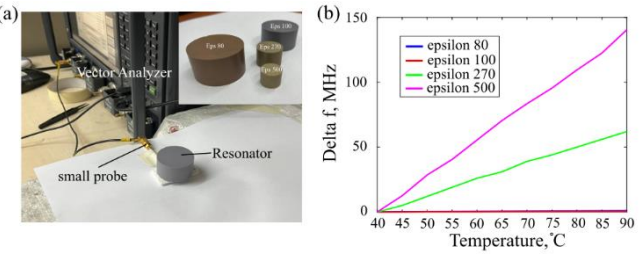

Fig. 3. (a) The photo of the setup to measure the resonance frequency of the manufactured resonators using a small loop antenna. The inset shows the photo of the fabricated devices. (b) The dependence of the resonance frequency shift on temperature. Different dielectric permittivities are in legends.

Fig. 3*b* demonstrates the TE01 mode resonance shift as a function of temperature for resonators with different permittivities. $BaTiO_3$ (ε = 500) has the strongest temperature dependence, resulting in a resonance shift of 3 MHz per 1°C. $SrTiO_3$ (ε = 270) is also quite sensitive with a resonance shift of 1.5 MHz per 1°C. These two materials are the best candidates among the materials, considered here. Other ceramics, based on TiO2-ZrO2 with permittivity of 80–100, are temperature stable and are less promising for sensing here.

A resonator with a permittivity of 500 was chosen for realizing the tag with the parameters obtained from the numerical model. To demonstrate the concept, measurements were conducted in an anechoic chamber. In a readout configuration (see the experiment layout in Fig. 4*a*), the tag's performance was tested. A commercial reader Impinj R2000 detected the tag at 4 meters. The communication channel with the RFID band was monitored via the software. The reader's antenna was a PCB-based Yagi-Uda design with four directors, offering -13 dB matching across the 850–900 MHz range and a gain of 7.5 dBi at 867 MHz. The transmission power level was set at 20 dBm. Measurements were conducted in Europe RFID band 865–868 MHz with communication channels of 500 KHz.

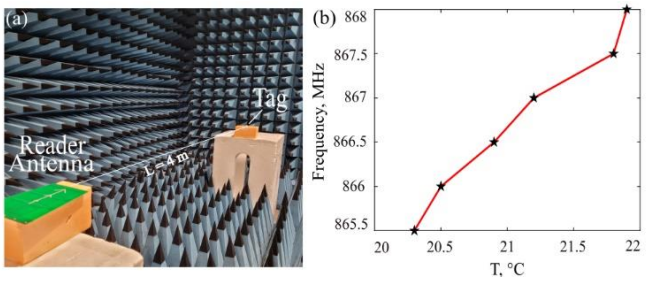

Fig. 4. (a) Photograph depicting the experimental setup inside the anechoic chamber. (b) The temperature-dependent central frequency of a communication channel, as acquired by the reader

Fig. 4*b* displays how the tag's response frequency varies with temperature. As the temperature increases, the tag's permittivity drops down, and thus the resonant frequency increases. The $BaTiO_3$ ceramic tag enables monitoring temperature changes that are less than one degree. The sensitivity can be further adjusted by choosing different ceramics and expanding the temperature range by using a broader RFID band, such as the USA 902-928 MHz with 50 or 100 communication channels. This will allow to obtain 50 or 100 measurement points, respectively.

IV. Conclusion

The experimental demonstration of environmental temperature monitoring was carried out using a compact RFID tag based on ceramic resonator. A key aspect of the design is the excitation of a fundamental magnetic dipole mode in a miniature cylindrical dielectric resonator. This mode is powered by a metallic split ring, which interacts with the resonator and incorporates an integrated RFID chip. It has been proposed to employ the frequency subcarriers of the interrogator to monitor temperature changes. The designed tag has a miniature size of $14.6 \times 14.6 \times 12\ mm^3$. A key benefit of this method is that it can be easily implemented without the use of supplementary equipment. Equipping high-index ceramic RFID tags with additional capabilities apart from their long reading ranges further promotes this technology in application to IoT and IoSM (Internet of Small Things), involving compact, budget-friendly, and resource-efficient units expected to handle various functions.

References

[1] K. Finkenzeller, *RFID Handbook*. 2000.

[2] D. Dobkin, The RF in RFID: Passive UHF RFID in Practice. Oxford: Elsevier, 2007.

[3] L. Atzori, A. Iera, and G. Morabito, "The Internet of Things: A survey," *Comput. Networks*, vol. 54, no. 15, pp. 2787–2805, Oct. 2010, doi: 10.1016/j.comnet.2010.05.010.

[4] H. Lasi, P. Fettke, H. G. Kemper, T. Feld, and M. Hoffmann, "Industry 4.0," *Bus. Inf. Syst. Eng.*, vol. 6, no. 4, pp. 239–242, Aug. 2014, doi: 10.1007/S12599-014-0334-4/FIGURES/1.

[5] I. Yusupov, D. Filonov, A. Bogdanov, P. Ginzburg, M. V. Rybin, and A. Slobozhanyuk, "Chipless wireless temperature sensor based on quasi-BIC resonance," *Appl. Phys. Lett.*, vol. 119, no. 19, p. 193504, Nov. 2021, doi: 10.1063/5.0064480.

[6] Y. Feng, L. Xie, Q. Chen, and L. R. Zheng, "Low-cost printed chipless RFID humidity sensor tag for intelligent packaging," *IEEE Sens. J.*, vol. 15, no. 6, pp. 3201–3208, Jun. 2015, doi: 10.1109/JSEN.2014.2385154.

[7] A. Beriain, I. Rebollo, I. Fernandez, J. F. Sevillano, and R. Berenguer, "A passive UHF RFID pressure sensor tag with a 7.27 bit and 5.47pJ capacitive sensor interface," *IEEE MTT-S Int. Microw. Symp. Dig.*, 2012, doi: 10.1109/MWSYM.2012.6258415.

[8] D. Dobrykh *et al.*, "Caramel UHF RFID Sensors for Pest Monitoring," *IEEE J. Radio Freq. Identif.*, vol. 7, pp. 601–608, 2023, doi: 10.1109/JRFID.2023.3334431.

[9] D. Dobrykh *et al.*, "Long-Range Miniaturized Ceramic RFID Tags," *IEEE Trans. Antennas Propag.*, vol. 69, no. 6, pp. 3125–3131, 2021, doi: 10.1109/TAP.2020.3037663.

[10] I. Yusupov, D. Dobrykh, D. Filonov, A. Slobozhanyuk, and P. Ginzburg, "Miniature Long-Range Ceramic On-Metal RFID Tag," *IEEE Trans. Antennas Propag.*, vol. 70, no. 11, pp. 10226–10232, Nov. 2022, doi: 10.1109/TAP.2022.3195551.

[11] D. Dobrykh, I. Yusupov, P. Ginzburg, A. Slobozhanyuk, and D. Filonov, "Self-aligning roly-poly RFID tag," *Sci. Reports 2022 121*, vol. 12, no. 1, pp. 1–7, Feb. 2022, doi: 10.1038/s41598-022-06061-6.

[12] D. Dobrykh, A. Maksimenko, I. Yusupov, D. Filonov, A. Slobozhanyuk, and P. Ginzburg, "Resonance cascading in a ceramic tag for long-range omnidirectional radio-frequency identification communication," *Phys. Rev. Appl.*, vol. 20, no. 6, p. 064022, Dec. 2023, doi: 10.1103/PHYSREVAPPLIED.20.064022/FIGURES/9/MEDIUM.